arXiv:1211.4922v1 [cond-mat.str-el] 21 Nov 2012

Unusual temperature dependence of the spectral weight near the Fermi level of $NdNiO_3$ thin films

E. F. Schwier[1], R. Scherwitzl[2], Z. Vydrovà[1], M. García-Fernández[1],
M. Gibert[2], P. Zubko[2], M. G. Garnier[1], J.-M. Triscone[2] and P. Aebi[1]
[1]*Département de Physique and Fribourg Center for Nanomaterials,*
University of Fribourg, CH-1700 Fribourg, Switzerland and
[2]*Département de Physique de la Matière Condensée, University of Geneva,*
24 Quai Ernest-Ansermet, CH-1211 Genève 4, Switzerland

We investigate the behavior of the spectral weight near the Fermi level of $NdNiO_3$ thin films as a function of temperature across the metal-to-insulator transition (MIT) by means of ultraviolet photoelectron spectroscopy. The spectral weight was found to exhibit thermal hysteresis, similar to that of the dc conductivity. A detailed analysis of the temperature dependence reveals two distinct regimes of spectral loss close to the Fermi level. The temperature evolution of one regime is found to be independent from the MIT.

I. INTRODUCTION

Nickel-based rare-earth perovskite oxides $R\mathrm{NiO}_3$, with R being a trivalent rare earth, are a model system to study temperature-driven metal-to-insulator transition (MIT). They are among the few oxide families that exhibit metallic conductivity and, except for $LaNiO_3$, all nickelates undergo an MIT with a critical temperature that depends on the radius of the rare-earth ion[1,2]. The MIT in the nickelates is accompanied by a structural transition from an orthorhombic (space group Pbnm)[3] to a monoclinic structure (space group $P2_1/n$)[4,5] with a Ni-O bond length disproportionation. The insulating phase is thought to exhibit charge order with two inequivalent Ni sites where the charge from the trivalent ion is split ($d^n d^n \rightarrow d^{n+\delta} d^{n-\delta}$) between two neighboring nickel sites[5–9]. For lighter rare earths like Nd and Pr the MIT is accompanied by a magnetic transition from a paramagnetic to an antiferromagnetic ground state with unusual spin order. For heavier rare earths the magnetic transition occurs at lower temperatures than the MIT[10,11].

The origin of the metal-insulator transition is currently under debate. The conduction band of $R\mathrm{NiO}_3$ is constituted by the covalent bonding of Ni 3d and O 2p orbitals. Initially, nickelates were located in the Zaanen-Sawatzky-Allen scheme[12] at the boundary between charge-transfer insulators and low-Δ metals[13]. Due to their small charge transfer energy Δ, it was argued that nickelates may even be considered as self-doped Mott insulators[14], where electrons are transferred from the oxygen to the nickel to form a $3d^8\underline{L}$ configuration ($\underline{L}$ denotes a hole in the oxygen ligand). Charge and spin order would then emerge naturally in these compounds[14,15]. Alternatively, charge ordering has been suggested to originate from a strong Hunds coupling, which would overcome the Coulomb interaction energy U and provide an alternative route to lift the orbital degeneracy in nickelates[16]. In this picture, nickelates were considered as band insulators rather than Mott insulators. In recent optical experiments, however, it was shown that Mott physics is essential to describe the redistribution of spectral weight[17]. Finally, recent dynamical mean field theory (DMFT) calculations[18] suggested that the Ni occupancy is not compatible with an insulating state caused by a Mott transition or charge transfer and that new physics beyond these frameworks might be needed to account for the insulating state in nickelates.

Ultraviolet photoelectron spectroscopy (UPS) is an ideal tool to probe the electronic structure and the effects of electronic correlations. The density of states (DOS) of the valence band is closely related to the measured photoelectron intensity (spectral weight), and changes in the latter can be related to the opening of a gap during the MIT[19], variation of the bandwidth[20] or the transfer of spectral weight between different parts of the valence band[21]. Photoemission measurements on $R\mathrm{NiO}_3$ have been performed on polycrystalline samples[22–26] as well as on thin films[27–30]. Measurements on thin films, however, were only conducted using the relatively low resolution x-ray photoemission spectroscopy (XPS). The present work represents the first high resolution UPS measurements on nickelate thin films.

In recent years the synthesis of nickelate thin films has become increasingly popular. Due to the absence of sufficiently large single crystals, epitaxial thin films are the closest system available to study the intrinsic properties of nickelates. In addition, films can be grown sufficiently thin to measure the influence of epitaxial strain on the phase transition[31–35], opening another degree of freedom in the exploration of the phase diagram of nickelates.

In this paper we present an analysis of the temperature dependence of the spectral weight near the Fermi level of $NdNiO_3$ thin films measured with UPS. We compare measurements at different temperatures from well above to well below the phase transition. We study changes in the valence band as well as the loss of spectral weight near the Fermi edge during the transition. The absence of a complete gap opening in the system is investigated by an analysis of the temperature dependent evolution of the spectral weight in the vicinity of the Fermi level. Finally, the loss of spectral weight is separated into two regimes: at and close to the Fermi energy, and reasons for their different-temperature evolutions are discussed.

II. EXPERIMENT

Epitaxial $NdNiO_3$ thin films were grown on (001)-oriented Nb:$SrTiO_3$ and $SrTiO_3$ substrates by radio-frequency off-axis magnetron sputtering in 0.180 mbar of an oxygen/argon mixture of ratio 1:3 at a substrate temperature of 490°C. More details on the growth conditions and structural characterization of $NdNiO_3$ films can be found in Ref.[36]. In this study, the film thickness was approximately 100 nm. DC transport measurements were carried out in a four-point configuration between room temperature and 4.2 K in a helium dipping station with a heating/cooling rate of approximately 1 K/min. Four platinum electrodes were deposited in each corner of the sample and the resistance R (or conductance $\sigma = 1/R$) was measured in constant current mode. The transition temperature T_{MIT} is defined as the temperature where $d(\ln R)/dT$ is maximum.

The ex-situ transferred films were cleaned from adsorbates by annealing in an oxygen atmosphere ($P_{O_2} \approx 200$ mbar) at $T \approx 750$ K for more than two hours. The surface cleanliness was tested using x-ray photoelectron spectroscopy of the C 1s core levels, whereas the quality of the atomic order at the surface could be verified by means of low electron energy diffraction.

The UPS spectra were recorded using an upgraded SCIENTA SES 200 analyzer. S-polarized monochromatic photons from the He I_α line ($h\nu = 21.2$ eV) of a helium discharge lamp were used to excite the photoelectrons. The base pressure in the chamber did not exceed $4{\times}10^{-11}$ mbar, while the He partial pressure during the measurement was below $5{\times}10^{-10}$ mbar. All spectra were recorded at normal emission with angular integration and with an energy resolution better than 8 meV. The position of the Fermi energy (E_F) was determined by fitting the spectral weight of sputtered polycrystalline Nb at a temperature of 17 K. The constant photon flux was verified manually during the measurements and the spectra are not normalized. The results were reproduced on different samples during multiple experiments.

Sample cooling and heating during the photoemission experiments was achieved by thermal contact with LHe and resistive heating of the manipulator at a rate of less than 2 K/min for the high resolution heating ramp and less than 4 K/min during the complete cooling and heating cycle. The samples remained at the lowest temperature for at least one hour before the heating commenced.

III. RESULTS & DISCUSSION

The valence band above and below T_{MIT}

In Fig. 1 the valence band of $NdNiO_3$ near E_F is plotted for two temperatures. The spectrum at 20 K (blue) corresponds to the antiferromagnetic insulating phase while the spectrum at room temperature (red) corresponds to the film being in the paramagnetic metallic phase. The inset shows the full valence band plotted for the same two temperatures. It is composed of several features (A-F).

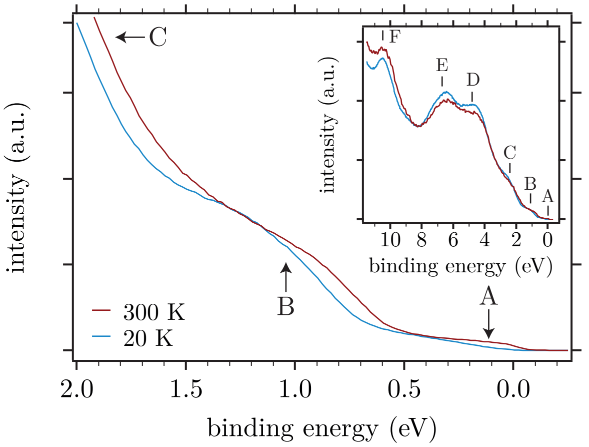

Figure 1: Region of the valence band near E_F above (red) and below (blue) the MIT as measured with He I_α. At E_F a loss of spectral weight is present (A), while at higher binding energies features in the spectral weight are shifted by approximately 0.2 eV (B & C). (Inset) The full valence band of $NdNiO_3$ at the same temperatures. Black bars mark the peak positions as determined from a second derivative of the low temperature spectrum.

The A region has been associated with the e_g^* band ($E_B < 400\,\mathrm{meV}$). It is situated in close proximity to E_F and its character is dominated by the strong hybridization of oxygen and nickel states[22,23,37]. Upon cooling the A region exhibits a strong loss of spectral weight from the metallic to the insulating phase. Such a behavior is consistent with previous photoemission measurements and has been linked to changes in the initial and final state configuration as well as to an opening of a charge-transfer gap[24–28].

The B peak ($E_B \approx 1$ eV) can be associated with the t_{2g}^* band of $NdNiO_3$. *Ab initio* calculations[22,37] propose a similar strength of orbital hybridization as in the A region. At lower temperatures, this feature is shifted by approximately 0.2 eV to higher binding energies. This is compatible with similar changes reported by Eguchi et *al.* who performed photoemission with a bulk-sensitive excitation energy of $h\nu = 7927$ eV[27]. The nature of this shift might be related to the transfer of spectral weight found in the manganite $Pr_{1/2}Sr_{1/2}MnO_3$ during the MIT[38], where a comparable shift of 0.2 eV is present.

The C peak ($E_B \approx 2.4$ eV) is expected to be composed of O 2p and, to a smaller part, of Ni 3d states[22,37]. Like the B peak, it also shifts by approximately 0.2 eV to higher binding energies. The comparable shifts of both the B and the C peaks suggest a similar driving force coupling to the binding energy of both features. A precise analysis of the shift of both bands as a function of temperature should provide additional information regarding this hypothesis.

The D peak ($E_B \approx 4.8$ eV) and E peak ($E_B \approx 6.7$ eV) are considered to be dominated by O 2p states, where, in the case of the D peak, localized Nd 4f states also contribute to the spectral weight[22,39]. At low temperatures both peaks slightly increase in intensity. It seems unlikely that this increase is related to additional adsorption of oxygen at the surface, as x-ray photoemission measurements of the O 1s core level do not show any increased emission at low temperatures. It should be noted that the E peak does exhibit a higher intensity compared to what is known from literature. A comparison of different publications shows that this feature is more prominent in thin films[27,28] than in polycrystalline samples[22,24,25]. This suggests, that the highly coordinated single-crystalline lattice of the thin film samples is a possible reason for this difference.

The F peak ($E_B \approx 10.5$ eV) can be identified, by comparison with $\mathrm{PrNiO_3}$, to be the result of a photoemission satellite with d^6 and $d^8\underline{L}^2$ character[23]. The suggestion by Galicka et *al.*[28] that a peak at this binding energy might be related to residual carbon at the surface of the sample can be ruled out in the present case due to the absence of C 1s in the XPS measurements. It should be noted that the peak is broadened towards higher binding energies in the insulating phase. Its satellite nature connects this broadening to a change in the electronic configuration of the valence electrons at E_F.

Energy distribution curves at different temperatures

In this paper the focus is set on the strong reduction of spectral weight in the e_g^* band (A region) crossing E_F. To investigate the intensity loss and its temperature dependence in this region, several high resolution spectra were recorded while the sample was heated from 10 K to ambient temperature.

In Fig. 2 the raw energy distribution curves (EDCs) recorded close to E_F at different temperatures have been plotted. The spectra were obtained during a heating cycle to ensure the fully insulating state of the sample at low temperatures[40]. A comparison between the highest ($T = 1.60T_{MIT}$) and lowest ($T = 0.06T_{MIT}$) temperature spectra shows a strong decrease of the spectral weight (A region) between binding energies of approximately 400 meV and E_F. Also visible is a region above 450 meV which exhibits a temperature dependent loss. The latter is, in fact, the tail of the B peak shifting to higher binding energies during the MIT (see Fig. 1). In order to highlight the evolution of spectral weight in the A region, the EDCs will be separated into two different temperature regimes: a low temperature regime where the sample is in a nominally insulating state, and a temperature regime around the MIT where coexistence of metallic and insulating domains is expected.

The spectra at temperatures up to 80 K do not exhibit any temperature dependence and between 80 K and 130 K only a very weak intensity increase is present. All spectra show a small but finite contribution of spectral weight at and above E_F without a resolvable Fermi edge. Also, an almost linear slope is present in the energy-dependent intensity across the whole A region.

The fact that no Fermi edge can be resolved in the low temperature spectra supports the notion of a fully insulating sample without metallic domains. However, there is no complete gap at E_F either, as demonstrated by the residual intensity present even at lowest temperatures. The presence of a gap is expected in the insulating state of a normal MIT. Its absence has to be interpreted as a sign of the unusual nature of the transition.

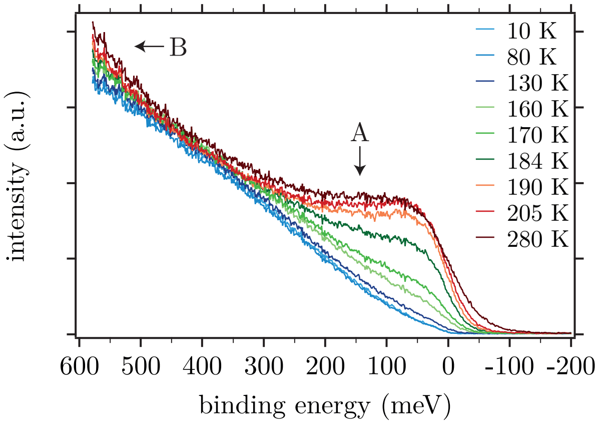

Figure 2: Angle-integrated energy distribution curves of the spectral weight close to E_F. The MIT is accompanied by an almost complete suppression of spectral weight at E_F as well as a loss of spectral weight at higher binding energies. Increased loss at 600 meV is caused by the shift of bands around 1 eV (see Fig.1).

It has been proposed that the abscence of a complete gap in the spectra may be the result of a highly assymetric gap broadended by experimental resolution[41]. The valence band onset in such a system would lie very close to but below E_F. The measurement process then leads to a convolution between the spectral function including the gap and the instrumental broadening. This, in turn, would result in a residual intensity at E_F in the low temperature spectra.

In Fig. 2 the onset of the resolution-broadened valence band can be estimated to lie between (-5 ± 3) meV (10 - 80 K) and (-25 ± 3) meV (130 K) in the insulating regime. The onset at the lowest temperature is compatible with our experimental resolution (8 meV). However, the onset at 130 K (-25 meV) cannot be explained by resolution broadening, meaning that the system cannot exhibit a complete gap in the insulating phase. This means that the loss of spectral weight has to be caused by a different process. There are several possible explanations for the observed evolution of the spectral weight.

Firstly, the MIT has to be understood as a transition from a metal to a semiconductor with a very low activation energy[42,43]. In this scenario there is a completely gapped Fermi surface but localized donor or acceptor states are present within the gap. These states, given a high enough density, can contribute to the total photoemission signal with a finite intensity in the photoemission spectra at E_F[44,45]. Also, a polaronic in-gap state has been proposed to be present in $La_{1/3}Sr_{2/3}FeO_3$[46] after the system undergoes a transition from a metallic to an insulating state with charge and spin order similar to $NdNiO_3$.

Secondly, in a manner similar to d-wave superconductors[47] or charge density wave compounds[48], only parts of the Fermi surface might actually be gapped, leaving bands crossing E_F to contribute to the spectral weight. The idea of a partially gapped Fermi surface is given support by the fact that optics experiments[17,49], indicate a gap opening in $NdNiO_3$ while only probing the band structure at the center of the Brillouin zone. In the presence of a Mott type transition this could lead to a zero-size gap[50], where residual density of states remains at temperatures lower than T_{MIT} due to an overlap of the upper and lower Hubbard bands at E_F[51]. Dardel et *al.*[52] were able to fit residual spectral weight below T_{MIT} in the Mott insulator TaS_2 using this framework. Similar fits, however, do not converge for the present data.

Another fascinating possibility was presented through calculations of Lee et *al.*[15] by an application of DMFT. They argued, that a bond-centered spin-density-wave state could be present in the low temperature phase of the nickelates. This leads to Dirac-cone-like bands crossing E_F with a linear density of states that would resemble the linear spectral weight present in our data. They predict the system to be semi-metallic in the presence of charge order. A gap is only formed if the orthorhombic distortion of the crystal becomes sufficiently high, which might be the case for heavier rare earths. So far, the hypothesis that a gap might emerge in the electronic structure under sufficiently large orthorhombic distortion could not be confirmed by photoemission measurements on $EuNiO_3$ and $SmNiO_3$[30,41].

At higher temperatures ($T > 160$ K), a Fermi edge becomes clearly visible in the spectra (Fig. 2) and can be fitted using a polynomial density of states. These fits result in a reasonable effective temperature as well as the correct position of E_F. The emergence of emission from metallic domains is to be expected at temperatures above the critical temperature of the phase transition $T_{1,low}$ (see Fig. 3 a). In addition to the emergence of a Fermi edge, the region between the two critical temperatures (see Fig. 3 a) of the MIT ($T \approx 160-200$ K) is marked by a sudden increase of the spectral weight that contributes approximately 2/3 of the total loss at E_F. These results are generally in good agreement with previous photoemission experiments on polycrystalline $R\mathrm{NiO}_3$ crystals.[24–27].

So far, the analysis of the EDCs strongly indicates that no complete gap is present in the electronic structure. It is, however, not clear if the loss of spectral weight in region A, as well as the residual intensity at E_F in the low temperature spectra, are the result of a pseudo gap, intensity from a tail of lower-lying O 2p states, donor levels inside the gap, a novel electronic state at low temperatures or a combination of the above. An answer to this question could be obtained by future angle resolved measurements which are able to resolve the dispersion of the electronic bands above and below the MIT.

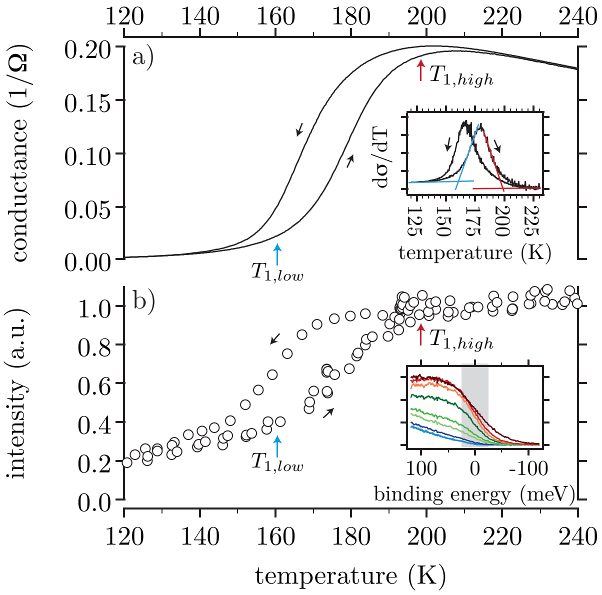

Figure 3: a) Conductance of $NdNiO_3$ as a function of temperature. The blue and red arrows mark the two critical temperatures of the hysteresis on heating, which are defined by the intersections of the blue and red lines in the inset. (Inset) Temperature derivative of the conductance. b) The integrated spectral weight at E_F as a function of temperature. The plot was normalized to the constant intensity above 250 K. (Inset) Energy distribution curves from Fig. 2 with the ± 25 meV interval around E_F used for integration.

Comparison of spectral weight and conductivity

Even in the absence of momentum resolved spectra it is still possible to shed further light on the behavior of the electronic states at E_F by comparing the evolution of the effective number of charge carriers with the actual conductivity of the sample. The presence of any kind of gap in the electronic structure is expected to result in a correlation between the transport data and the integrated spectral weight at the Fermi level[53].

In Fig. 3, the thin film conductance (Fig. 3 a) is compared to the integrated spectral weight at E_F (Fig. 3 b) as a function of temperature in a window around T_{MIT}. The top inset shows the temperature derivative of the conductance used to define the critical temperatures of the transition $T_{1,low}$ & $T_{1,high}$. The bottom inset illustrates the energy window used to obtain the integrated spectral weight.

The conductance (Fig. 3 a) exhibits a narrow hysteresis ($\Delta T \approx 13$ K) with the MIT temperatures of $T_{MIT} = T_{MIT,\uparrow} = 179$ K on heating and $T_{MIT,\downarrow} = 166$ K on cooling (inset in Fig. 3 a). To quantify the extent of the MIT, we define the critical temperatures $T_{1,low}$ and $T_{1,high}$ for the heating branch. These are estimated as shown in the top inset of Fig. 3 a) to be $T_{1,low} \approx 160$ K and $T_{1,high} \approx 200$ K from the intersection of the blue and red lines respectively. These temperatures mark sharp changes in the conductivity data and thus roughly quantify the boundaries for the phase coexistence region or percolation thresholds for the metallic and insulating states.

The integrated photoemission intensity in Fig. 3 b) is also hysteretic, with critical temperatures that are comparable[54] to the values determined from transport. By analogy with the thermal hysteresis in conductivity[43], the observed temperature hysteresis in the spectral weight implies the coexistence of metallic and semiconducting domains during the transition, both contributing individually to the photoemission signal. The determination of T_{MIT} by means of an analysis of the integrated spectral weight has been successfully performed on polycrystalline $PrNiO_3$[55]. In this work, however, it was possible for the first time to resolve the hysteresis in these systems.

It should be noted that hysteretic behavior has been reported for several other system parameters associated with the MIT. Among these are the temperature dependence of the magnetic moment at the nickel site[2,56,57], the unit cell volume[58], as well as transport properties like the Seebeck coefficient and the resistivity[59]. The hysteresis in the photoemission data is a demonstration that the MIT is indeed responsible for the loss of spectral weight at E_F.

Temperature-dependent loss of spectral weight

Since the loss of spectral weight at E_F can be connected to the MIT, we will now perform a closer analysis of its temperature and binding energy dependence in the A region.

In Fig. 4 the integrated intensity at different binding energies within the A region has been plotted as temperature distribution curves (TDCs) obtained during a heating ramp. The intensity was integrated within windows of ± 25 meV around the annotated binding energies. A variation of this integration window between ± 3 meV and ± 100 meV did not lead to a qualitative change of the plot. The curves have been offset against each other for clarity as the room temperature intensities are similar over a broad range of binding energies.

In the vicinity of E_F the strongest feature is the sudden increase of intensity around T_{MIT} between the critical temperatures of the MIT $T_{1,low}$ and $T_{1,high}$ (blue and red dashed lines). This feature completely disappears at higher binding energies where only a linear increase of the spectral weight is present over a broad temperature range (see 300 meV curve).

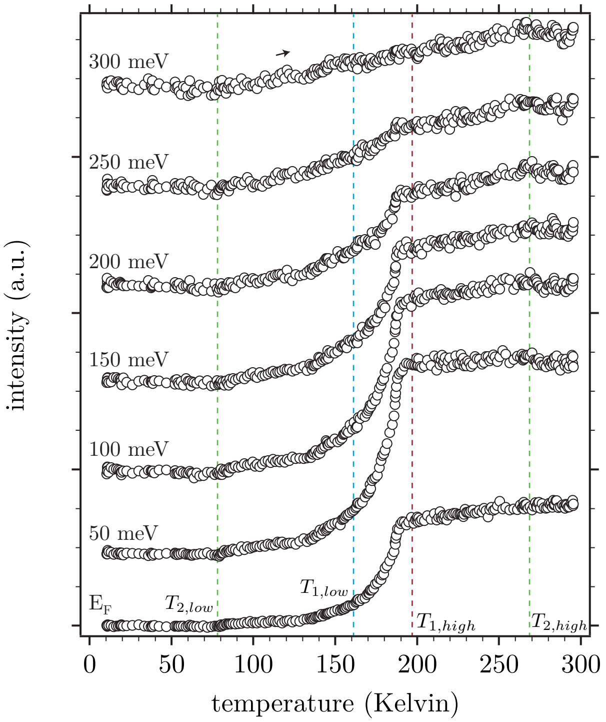

Figure 4: Spectral weight integrated over a ± 25 meV window around various binding energies close to E_F as a function of temperature while heating the sample. The blue and red dashed lines denote the critical temperatures of the MIT on heating ($T_{1,low}$ & $T_{1,high}$) as obtained from the transport data. The green dashed lines ($T_{2,low}$ & $T_{2,high}$) act as guides to the eye for the changes in slope in the TDCs around 80 and 270 K, most prominent at higher binding energies.

The sudden increase of intensity around the MIT, as well as the absence of a similarly abrupt intensity change in the high binding energy region of the spectral loss, strongly suggest that the overall temperature evolution within the A region is actually governed by two regimes (A_1 & A_2) with distinct temperature dependences.

The fingerprint of the first regime A_1 is the sharp rise of intensity during the MIT between 160 and 200 K ($T_{1,low}$ & $T_{1,high}$ in Fig. 4). It is most prominent around E_F and its contribution to the total spectral loss vanishes almost completely around binding energies of 250 meV. The correlation between the intensity loss of A_1 close to E_F and the MIT was already demonstrated during the comparison of the integrated spectral weight at E_F with the conductivity of the sample (see Fig. 3). Further support is given by the comparison of the temperature dependence of A_1 with the effective number of charge carries determined from the integration of the optical conductivity by Katsufuji et *al.*[49]. They observed a sudden increase in effective carrier density around 150 K and a saturation at 200 K, which is consistent with the temperature dependence of A_1 observed in this work, despite the lower temperature resolution of the optical conductivity measurements. It is therefore evident that A_1 is directly connected to the physics of the MIT.

The second regime A_2 is governed by the linear increase of intensity over a broad temperature range. The intersections of linear fits are at $T_{2,low} \approx 80$ K and $T_{2,high} \approx 270$ K for characteristic temperatures of the linear increase at a binding energy of 300 meV (green dashed lines). These temperatures are, in fact, found to mark a change of the intensity evolution in all TDCs up to E_F. The similarity of the characteristic temperatures in TDCs at all binding energies gives support to the idea that the A_2 loss is not only confined to higher binding energies ($E_B \approx 300$ meV), but that A_2 also governs the temperature evolution at E_F within its respective temperature range together with A_1[60].

A comparison of the characteristic temperatures of A_2 ($T_{2,low}$ & $T_{2,high}$) with those of the MIT ($T_{1,low}$, T_{MIT} & $T_{1,high}$) shows that changes in the TDC that are attributed to A_2 are located far away from the MIT and therefore cannot be linked to the phase transition. A connection between A_2 and B can also be ruled out, as the temperature dependence of the B region is similar to that of A_1[61]. Another yet unknown process has to govern the temperature evolution of A_2. In this regard it is interesting to note that both temperatures ($T_{2,low}$ & $T_{2,high}$) are in close proximity to the temperatures reported to be related to changes in the magnetic properties of the system. At a temperature comparable to $T_{2,low}$ for instance , Mallik et *al.*[62] found a change in the sign of the magnetoresistance of $NdNiO_3$. At temperatures higher than T_{MIT} in the itinerant phase, the evolution of the magnetic moment at the Ni site has been extrapolated to yield a virtual Néel temperature at around 250 K (neutron diffraction)[10,41] or 230 K (Mössbauer effect)[56]. The latter study also proposed magnons to be present at least in the low temperature regime of the system. The several hundred meV binding energy range of the A_2 regime is also compatible with the range of magnon dispersion[63]. Also, the presence of a virtual Néel temperature has been suggested[64] to be reflected in a change of slope in the susceptibility measured by Zhou et *al.*[65] hinting at a magnetic transition in the itinerant phase.

Although no direct proof of a correlation between magnetic properties and electronic structure in the nickelates can be obtained from our data, the possibility that the observed loss A_2 is of magnetic origin certainly merits further study. The correlation between spectral weight and magnetic fluctuations has already been discussed by Kampf et *al.* for the metallic pseudogap phase of the cuprates[66]. Future measurements should therefore focus on changes in the electronic structure around these temperatures. Employing techniques other than photoemission, which are sensitive to the magnetic properties of the system, would provide usefull information.

IV. CONCLUSION

By measuring the temperature evolution of the valence band of $NdNiO_3$ thin films, we were able to highlight the subtle changes in the electronic structure of $NdNiO_3$ thin films as a function of temperature. We could further demonstrate the presence of thermal hysteresis in the spectral weight at the Fermi level and relate its evolution to the conductivity of the thin film. The large temperature range investigated together with the high temperature and energy resolution allowed us to distinguish two different loss regimes within the spectral weight close to E_F.

The first regime could be directly related to changes induced by the MIT. Several possible mechanisms responsible for the MIT and the existence of residual intensity at E_F in the insulating phase were discussed. By analyzing the temperature evolution of the spectral weight at various binding energies, a second regime could be identified, which was shown to be completely disconnected from the MIT, with characteristic temperatures for the loss of spectral weight far above and below T_{MIT}. After comparison with measurements sensitive to magnetic structure, it was suggested that changes in the magnetic state of the system could be responsible for this interesting temperature behavior.

Acknowledgments

The authors would like to thank A. J. Millis, D. Baeriswyl, V. K. Malik, C. Battaglia and C. Didiot for helpful discussions as well as the mechanics and electronics workshops in Fribourg and Geneva for their support.

This project was supported by the Fonds National Suisse pour la Recherche Scientifique through Division II and the Swiss National Center of Competence in Research MaNEP.

---

[1] J. B. Torrance, P. Lacorre, A. I. Nazzal, E. J. Ansaldo, and C. Niedermayer, Physical Review B **45**, 8209 (1992).

[2] M. Medarde, Journal of Physics: Condensed Matter **9**, 1679 (1997).

[3] J. L. Garcia-Munoz, J. Rodriguez-Carvajal, P. Lacorre, and J. B. Torrance, Physical Review B **46**, 4414 (1992).

[4] J. A. Alonso, M. J. Martinez-Lope, M. T. Casais, M. G. A. Aranda, and M. Fernandez-Diaz, Journal of the American Chemical Society **121**, 4754 (1999).

[5] U. Staub, G. I. Meijer, F. Fauth, R. Allenspach, J. G. Bednorz, J. Karpinski, S. M. Kazakov, L. Paolasini, and F. d'Acapito, Physical Review Letters **88**, 126402 (2002).

[6] J. A. Alonso, J. L. Garcia-Munoz, M. T. Fernandez-Diaz, M. A. G. Aranda, M. J. Martinez-Lope, and M. T. Casais, Physical Review Letters **82**, 3871 (1999).

[7] J. A. Alonso, M. J. Martinez-Lope, M. T. Casais, J. L. Garcia-Munoz, and M. T. Fernandez-Diaz, Physical Review B **61**, 1756 (2000).

[8] V. Scagnoli, U. Staub, M. Janousch, A. Mulders, M. Shi, G. I. Meijer, S. Rosenkranz, S. Wilkins, L. Paolasini, J. Karpinski, et al., Physical Review B **72**, 155111 (2005).

[9] M. Medarde, C. Dallera, M. Grioni, B. Delley, F. Vernay, J. Mesot, M. Sikora, J. A. Alonso, and M. J. Martinez-Lope, Physical Review B **80**, 245105 (2009).

[10] J. L. Garcia-Munoz, J. Rodriguez-Carvajal, and P. Lacorre, Physical Review B **50**, 978 (1994).

[11] V. Scagnoli, U. Staub, Y. Bodenthin, M. Garcia-Fernandez, A. M. Mulders, G. I. Meijer, and G. Hammerl, Physical Review B **77**, 115138 (2008).

[12] J. Zaanen, G. A. Sawatzky, and J. W. Allen, Physical Review Letters **55**, 418 (1985).

[13] J.B. Torrance and R. M. Metzger, Physica C: Superconductivity **182**, 351 (1991).

[14] T. Mizokawa, D. I. Khomskii, and G. A. Sawatzky, Physical Review B **61**, 11263 (2000).

[15] S. B. Lee, R. Chen, and L. Balents, Physical Review B **84**, 165119 (2011).

[16] I. I. Mazin, D. I. Khomskii, R. Lengsdorf, J. A. Alonso, W. G. Marshall, R. M. Ibberson, A. Podlesnyak, M. J. Martinez-Lope, and M. M. Abd-Elmeguid, Physical Review Letters **98**, 176406 (2007).

[17] M. K. Stewart, J. Liu, M. Kareev, J. Chakhalian, and D. N. Basov, Physical Review Letters **107**, 176401 (2011).

[18] H. Park, A. J. Millis, and C. A. Marianetti, Physical Review Letters **109**, 156402 (2012).

[19] T. Mizokawa, H. Namatame, A. Fujimori, K. Akeyama, H. Kondoh, H. Kuroda, and N. Kosugi, Physical Review Letters **67**, 1638 (1991).

[20] J. S. Kang, D. W. Hwang, C. G. Olson, S. J. Youn, K. C. Kang, and B. I. Min, Physical Review B **56**, 10605 (1997).

[21] C. Monney, E. F. Schwier, M. G. Garnier, N. Mariotti, C. Didiot, H. Cercellier, J. Marcus, H. Berger, A. Titov, H. Beck, et al., New Journal Of Physics **12**, 125019 (2010).

[22] S. R. Barman, A. Chainani, and D. D. Sarma, Physical Review B **49**, 8475 (1994).

[23] T. Mizokawa, A. Fujimori, T. Arima, Y. Tokura, N. Mōri, and J. Akimitsu, Physical Review B **52**, 13865 (1995).

[24] M. Medarde, D. Purdie, M. Grioni, M. Hengsberger, Y. Baer, and P. Lacorre, EPL (Europhysics Letters) **37**, 483 (1997).

[25] I. Vobornik, L. Perfetti, M. Zacchigna, M. Grioni, G. Margaritondo, J. Mesot, M. Medarde, and P. Lacorre, Physical Review B **60**, 8426 (1999).

[26] K. Okazaki, T. Mizokawa, A. Fujimori, E. V. Sampathkumaran, M. J. Martinez-Lope, and J. A. Alonso, Physical Review B **67**, 073101 (2003).

[27] R. Eguchi, Y. Okamoto, Z. Hiroi, S. Shin, A. Chainani, Y. Tanaka, M. Matsunami, Y. Takata, Y. Nishino, K. Tamasaku, et al., Journal of Applied Physics **105**, 056103 (2009).

[28] K. Galicka, J. Szade, P. Ruello, P. Laffez, and A. Ratuszna, Applied Surface Science **255**, 4355 (2009).

[29] A. X. Gray, A. Janotti, J. Son, J. M. Lebeau, S. Ueda, Y. Yamashita, K. Kobayashi, A. M. Kaiser, R. Sutarto, H. Wadati, et al., Physical Review B **84**, 075104 (2011).

[30] K. Bilewska, E. Wolna, M. Edely, P. Ruello, and J. Szade, Physical Review B **82**, 165105 (2010).

[31] A. Tiwari, C. Jin, and J. Narayan, Applied Physics Letters **80**, 4039 (2002).

[32] J. DeNatale and P. Kobrin, Journal of Materials Research **10**, 2992 (1995).

[33] G. Catalan, R. M. Bowman, and J. M. Gregg, Journal of Applied Physics **87**, 606 (2000).

[34] M. A. Novojilov, O. Y. Gorbenko, I. E. Graboy, A. R. Kaul, H. W. Zandbergen, N. A. Babushkina, and L. M. Belova, Applied Physics Letters **76**, 2041 (2000).

[35] A. Tiwari, C. Jin, and J. Narayan, Appl. Phys. Lett. **80**, 4039 (2002).

[36] R. Scherwitzl, P. Zubko, I. G. Lezama, S. Ono, A. F. Morpurgo, G. Catalan, and J.-M. Triscone, Advanced Materials **22**, 5517 (2010).

[37] D. Sarma, N. Shanthi, and P. Mahadevan, Journal of Physics: Condensed Matter **6**, 10467 (1994).

[38] A. Chainani, H. Kumigashira, T. Takahashi, Y. Tomioka, H. Kuwahara, and Y. Tokura, Physical Review B **56**, R15513 (1997).

[39] D. Sarma and C. Rao, Journal of Electron Spectroscopy and Related Phenomena **20**, 25 (1980).

[40] D. Kumar, K. P. Rajeev, J. A. Alonso, and M. J. Martinez-Lope, Journal of Physics: Condensed Matter **21**, 185402 (2009).

[41] I. Vobornik, PhD Thesis - École Polythechnique Fédérale de Lausanne (Switzerland) (1999).

[42] X. Granados, J. Fontcuberta, X. Obradors, L. Manosa, and J.B. Torrance, Physical Review B **48**, 11666 (1993).

[43] G. Catalan, R. M. Bowman, and J. M. Gregg, Physical Review B **62**, 7892 (2000).

[44] T. Higuchi, T. Tsukamoto, N. Sata, M. Ishigame, Y. Tezuka, and S. Shin, Physical Review B **57**, 6978 (1998).

[45] Y. Aiura, I. Hase, H. Bando, T. Yasue, T. Saitoh, and D. Dessau, Surface Science **515**, 61 (2002).

[46] H. Wadati, A. Chikamatsu, M. Takizawa, R. Hashimoto, H. Kumigashira, T. Yoshida, T. Mizokawa, A. Fujimori, M. Oshima, M. Lippmaa, M. Kawasaki,and H. Koinuma, Physical Review B **74**, 115114 (2006).

[47] A. Damascelli and Z.-X. Shen, Reviews of Modern Physics **75**, 473 (2003).

[48] V. Brouet, W. L. Yang, X. J. Zhou, Z. Hussain, N. Ru, K. Y. Shin, I. R. Fisher, and Z. X. Shen, Physical Review Letters **93**, 126405 (2004).

[49] T. Katsufuji, Y. Okimoto, T. Arima, Y. Tokura, and J.B. Torrance, Physical Review B **51**, 4830 (1995).

[50] P. Fazekas and E. Tosatti, Physica B+C **99**, 183 (1980).

[51] D. J. Thouless, Le Journal de Physique Colloques **37**, C4 (1976).

[52] B. Dardel, M. Grioni, D. Malterre, P. Weibel, Y. Baer, and F. Lévy, Physical Review B **45**, 1462 (1992).

[53] B. Dardel, M. Grioni, D. Malterre, P. Weibel, Y. Baer, and F. Lévy, Physical Review B **46**, 7407 (1992).

[54] Note the measured temperatures used for the photoemission data are offset from the actual sample temperatures due to the difference in heat conductance between LHe-thermocouple and LHe-sample, respectively.

[55] M. Medarde, A. Fontaine, J. L. Garcia-Munoz, J. Rodriguez-Carvajal, M. DeSantis, M. Sacchi, G. Rossi, and P. Lacorre, Physical Review B **46**, 14975 (1992).

[56] A. Caytuero, H. Micklitz, F. J. Litterst, E. M. Baggio-Saitovitch, M. M. Abd-Elmeguid, and J. A. Alonso, Physical Review B **74**, 094433 (2006).

[57] V. Scagnoli, U. Staub, A. M. Mulders, M. Janousch, G. I. Meijer, G. Hammerl, J. M. Tonnerre, and N. Stojic, Physical Review B **73**, 100409 (2006).

[58] P. Ruello, B. Perrin, T. Pezeril, V. Gusev, S. Gougeon, N. Chigarev, P. Laffez, P. Picart, D. Mounier, and J. Breteau, Physica B: Condensed Matter **363**, 43 (2005).

[59] X. Granados, J. Fontcuberta, X. Obradors, and J. B. Torrance, Physical Review B **46**, 15683 (1992).

[60] A change of intensity due to de- and adsorbtion of residual gas layers during the temperature ramp can be ruled out as temperature dependent desorbtion processes are typically confined to much smaller time and temperature scales due to the activated nature of the desorption.

[61] Unpublished work.

[62] R. Mallik, E. Sampathkumaran, J. A. Alonso, and M. Martinez-Lope, Journal of Physics: Condensed Matter **10**, 3969 (1998).

[63] J. Y. P. Delannoy, M. J. P. Gingras, P. C. W. Holdsworth, and A. M. S. Tremblay, Physical Review B **79**, 235130 (2009).

[64] G. Catalan, Phase Transitions **81**, 729 (2008).

[65] J. S. Zhou, J. B. Goodenough, B. Dabrowski, P. W. Klamut, and Z. Bukowski, Physical Review Letters **84**, 526 (2000).

[66] A. P. Kampf, and J. R. Schrieffer Physical Review B **42**, 7967 (1990).